Journal of ELECTRONIC MATERIALS, Vol. 41, No. 9, 2012
DOI: 10.1007/s11664-012-2156-9
© 2012 TMS

Gap Size Effects on the Shear Strength of Sn/Cu and Sn/FeNi Solder Joints

CAI CHEN,[1] LEI ZHANG,[1,2] JIAXI ZHAO,[1] LIHUA CAO,[1] and J.K. SHANG[1]

1.—Shenyang National Laboratory for Materials Science, Institute of Metal Research, Chinese Academy of Sciences, Shenyang 110016, China. 2.—e-mail: lzhang@imr.ac.cn

The effect of the gap size on the shear strength of a solder joint was investigated in both Sn/Cu and Sn/FeNi lap solder joints by varying the gap size from 20 μm to 300 μm. In the Sn/FeNi joints, the shear strength remained relatively constant, around 14 MPa, independent of the gap size. In contrast, the shear strength of the Sn/Cu joint decreased about 20% from 25 MPa to 20 MPa. The decrease was shown to result from Cu_6Sn_5 precipitation in the thicker Sn/Cu joint, which was absent in the thinner joints.

Key words: Solder, size effect, shear strength, microstructure

INTRODUCTION

Strength and plasticity are two main issues central to the mechanical reliability of a solder joint. They are often examined using common joint geometries, such as butt joint and lap joint. Since the stress state and deformation process in the joint are highly dependent on the geometry of the joint,[1,2] it is important that the effects of each geometrical parameter be understood clearly. Among the various geometrical parameters, the gap size, or the thickness of the bond, is most interesting in that it not only influences the mechanical state in the solder bond, but also impacts the microstructure within the joint, especially when the gap size is comparable to microstructural dimensions, such as grain size, or diffusion lengths of major diffusing species. While the mechanical aspect of the gap size effect has been well studied previously,[3] the microstructural effects have not been thoroughly investigated. This is unfortunate since dimensions of solder joints have decreased rapidly over the past few years to become comparable to microstructural dimensions.[4,5]

The mechanical aspect of the gap size was well described by Orowan,[3] who found that the yield strength or fracture strength of a butt brazed or soldered joint depended on a geometrical factor d/t, where d is the solder width and t is the gap size. Orowan's finding may be approximated using the following equation:[6]

$$\sigma_F = \sigma_{UTS/yield} \times (1 + d/6t), \quad (1)$$

where $\sigma_{UTS/yield}$ is the yield strength or ultimate tensile strength of the bulk solder. Such a gap size effect was normally recognized as a constraint effect originating from the differences of the mechanical properties between the Cu substrate and the solder, such as elastic modulus and Poisson's ratio. The lateral contraction of the solder near the interface is confined during deformation, resulting in a hydrostatic stress state and an increase in the joint tensile strength.

However, ambiguities exist regarding whether there is a gap-size-induced constraint effect on shear strength. Shen et al.[7,8] used lap shear Sn-3.5Ag/Cu solder joints with gap sizes ranging form 40 μm to 520 μm, and found that the ultimate shear strength (USS) appeared to be independent of the solder thickness. On the other hand, Zimprich and Cugnoni[9–12] reported that a strong increase of shear strength occurs when the gap size decreases from 326 μm to 156 μm in Sn-3.5Ag/Cu lap shear joints. Yang et al.[13] also showed that the shear strength increases rapidly with decreasing solder volume, when the fracture mode is primarily within the bulk solder. They pointed out that the difference in the microstructure arises from the faster cooling rate of solder balls with smaller volume, which might lead to strengthening of the solder joint.

(Received February 27, 2012; accepted May 24, 2012; published online June 13, 2012)

Unfortunately, details of the joint microstructure were not presented. More recently, Tian et al.[14] studied the bump size effect on deformation and fracture behavior of Sn-3.0Ag-0.5Cu/Cu solder joints during shear testing and suggested that the morphology and distribution of intermetallic compounds were the main reasons for the size effect.

To clarify the ambiguous understanding of the gap size effect on shear strength, this work was carried out to investigate the shear behavior of two types of solder joints. One was the Sn/Cu system where the Cu diffusion leads to not only fast intermetallic growth at the interface but also formation of Cu-Sn intermetallic in the solder. The other was made from the Sn/FeNi system in which the interfacial reaction is limited so structural complications induced by the formation of intermetallic compound can be minimized. No gap size effect was found in the FeNi/Sn system, but a strong gap size effect was observed in the Sn/Cu system. Both microstructural characterization and finite-element analysis were conducted to clarify the gap size effect on the lap shear strength of the solder joints.

EXPERIMENTAL PROCEDURES

The dimensions of the lap shear sample are shown in Fig. 1. A trench with area of 5 mm × 5 mm was machined on one side of the Cu sheet. The depth was controlled for the designed gap size. The surface of the trench was electrolytically polished and coated with RMA flux. Sn foil with purity of 99.9% was placed on one trench, facing upward. Then, the other Cu sheet with the same trench facing downward was placed on top. During the soldering process, the wetting force pulled the upper block sideways to form a solder joint. This self-restoring process driven by the wetting forces helped to eliminate defects such as pores and flux residue. After dwelling at 280°C for 40 s, the soldered lap shear joint was quickly quenched in water. To make Sn/FeNi solder joints, 58 wt.% FeNi alloy was electroplated to thickness of 3 μm on the Cu substrate after the Cu block was electropolished following the procedure by Guo.[15] The soldering process was the same as the one used for the Sn/Cu solder joint.

After soldering, the excess Sn and Cu were machined off to keep the overlap width at 3.0 mm, and the block was cut into four strips with the dimensions shown in Fig. 1. The strip samples were ground with abrasive paper and polished with 1-μm diamond suspensions. The thicknesses of the lap shear samples and the interfacial intermetallic compound (IMC) were examined by scanning electron microscopy (SEM, FEI Quanta 600) with energy-dispersive spectrometry (EDS) for composition identification.

The shear test was performed on a 2KN INSTRON 5848 tensile machine. Load–displacement curves were recorded automatically. Shear displacement was obtained directly from the crosshead movement. The strain rate was calculated as the displacement rate in the loading direction divided by the gap size. Strain rate of 10^{-3}/s was used for all samples with different gap sizes. Note that, for joints with larger gap sizes, higher displacement rates had to be used. For each condition, four specimens were tested and the average results from them are reported.

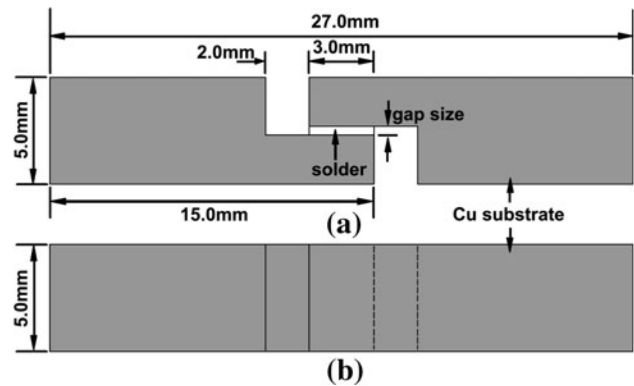

Fig. 1. Schematics of lap shear joint: (a) top view and (b) side view.

RESULTS

Microstructure of As-Fabricated Solder Joints

A side view of the as-soldered lap shear Sn/Cu joint is shown in Fig. 2. No obvious flaws or porosities can be seen, even for the joints with a very small gap of 20 μm. The joint has uniform clearance. The Sn/Cu interface was even and smooth, and covered with a Cu_6Sn_5 layer about 3 μm thick. The Sn/FeNi solder joint also exhibited good uniformity but with much thinner interfacial intermetallics.

In the 300-μm Sn/Cu solder joint, as shown in Fig. 3a, b, the Sn/Cu joint microstructure was dendrites surrounded by (Sn + Cu_6Sn_5) eutectic, which was common in the Sn/Cu soldering. There were also some columnar Sn dendrites growing normal to the Sn/Cu interface. However, as the joint gap was reduced to 20 μm, only one layer of Sn grains was formed in the Sn/Cu joint and no obvious eutectic phase or Cu_6Sn_5 particles could be observed. The composition analysis found Cu content of 1.3 ± 0.3 wt.%, 1.4 ± 0.3 wt.%, 1.3 ± 0.4 wt.%, and 1.8 ± 0.3 wt.% for the 300-μm, 100-μm, 50-μm, and 20-μm solder joints, respectively. The thickness of the Cu_6Sn_5 IMC at the Sn/Cu interface was the same for all gap sizes.

The Sn/FeNi joint microstructure is shown in Fig. 3c, d. The composition of the FeNi plating was close to that of invar alloy (64Fe-36Ni in wt.%). The IMC at the Sn/FeNi interface was primarily a layer of fine $FeSn_2$ grains, as in previous reports.[16,17] Due to the slow growth rate of $FeSn_2$, the thickness of IMC after reflow was less than 1 μm, much thinner than for the Sn/Cu reaction couple.[18] The solder

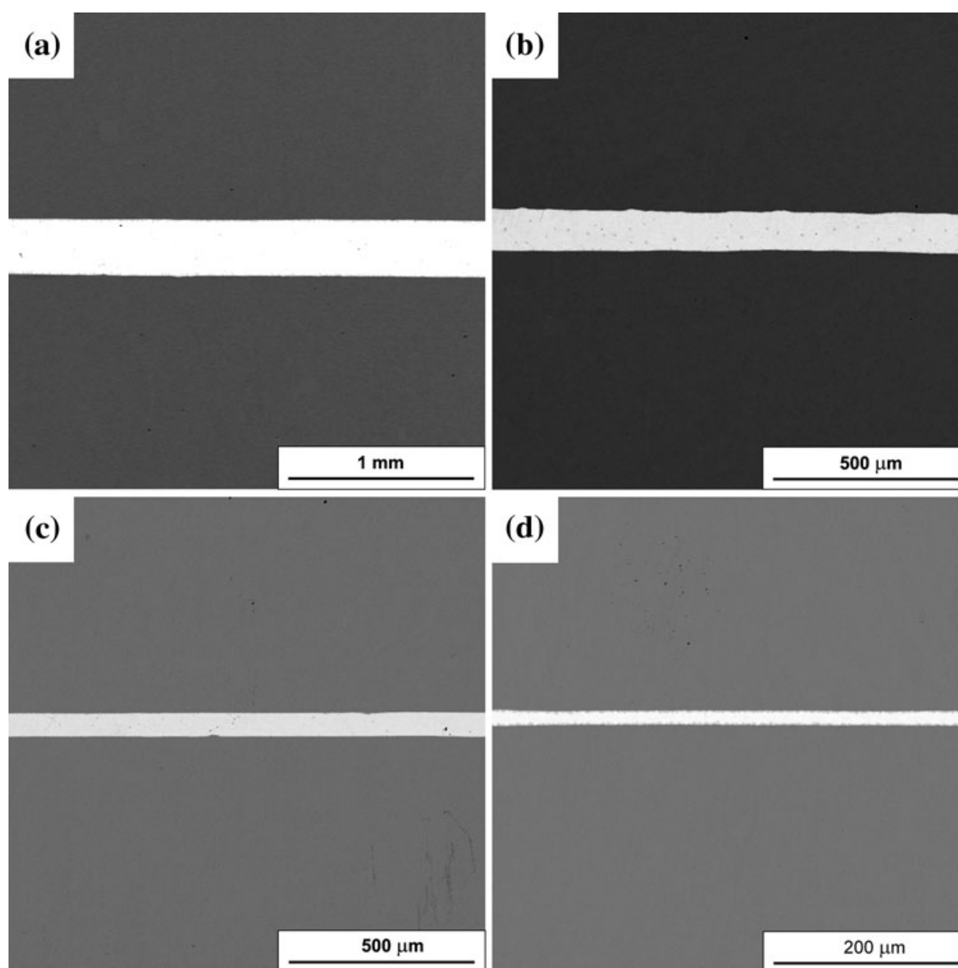

Fig. 2. Side views of Sn/Cu solder joints with different gap sizes: (a) 300 μm, (b) 100 μm, (c) 50 μm, and (d) 20 μm. The bright phase is the solder.

joint contained a single β-Sn phase. The SEM images exhibited a uniform grain size distribution within the whole joint regardless of the gap size. The content of Fe and Ni in the solder was lower than 0.2 wt.%, meaning that the solder bond was essentially made of pure Sn.

Shear Properties and Gap Size Effect on Sn/Cu and Sn/FeNi Solder Joints

The shear responses of Sn/Cu solder joints with different gap sizes are shown in Fig. 4a. The shear curves showed the same shape. The failure displacement decreased as the gap size decreased. For the Sn/FeNi solder joints with different gap sizes, the shear properties are shown in Fig. 4b. The 300-μm joints seemed to have slower work-hardening rate than the 20-μm and 50-μm joints, and the fracture displacement was also increased for the joint with larger gap size.

The USSs as a function of gap size for the Sn/Cu and Sn/FeNi joints are plotted in Fig. 4c. The joint with 20-μm gap showed only 80% of the strength of that with a 300-μm gap. However, for Sn/FeNi joints with different gap sizes, the USSs were around 14 MPa, although there was a slight drop for the joint with a 300-μm gap. When using a higher strain rate of 10^{-1}/s, the USS of the Sn/FeNi joint was almost the same: 26.5 ± 1.4 MPa for the 300-μm joint and 27.0 ± 1.5 MPa for the 20-μm joint. By comparison, the shear strength of a Sn/Cu joint soldered at 250°C for 1 min was reported to be about 15.4 ± 3.1 MPa by Tomlinson et al.[19]

The Vickers hardness of the Sn/Cu and Sn/FeNi solder joints was examined to see if there was any gap size effect on the solder intrinsic strength. In Fig. 4d, it is clear that the gap size had little influence on the HV hardness of the solder joints. For the Sn/Cu solder joints with gap from 300 μm to 50 μm, the HV hardness was around 13.3 kg/mm^2, whereas for the Sn/FeNi joints the hardness was around 9.2 kg/mm^2. Unfortunately, the Vickers test could not give the hardness value for the joint with gap of 20 μm, since the diagonal of the HV indentation exceeded the joint clearance. The HV hardness for a solder is normally determined by the solute concentration along with the size and distribution of IMC particles in the solder. Pure Sn solder is softer

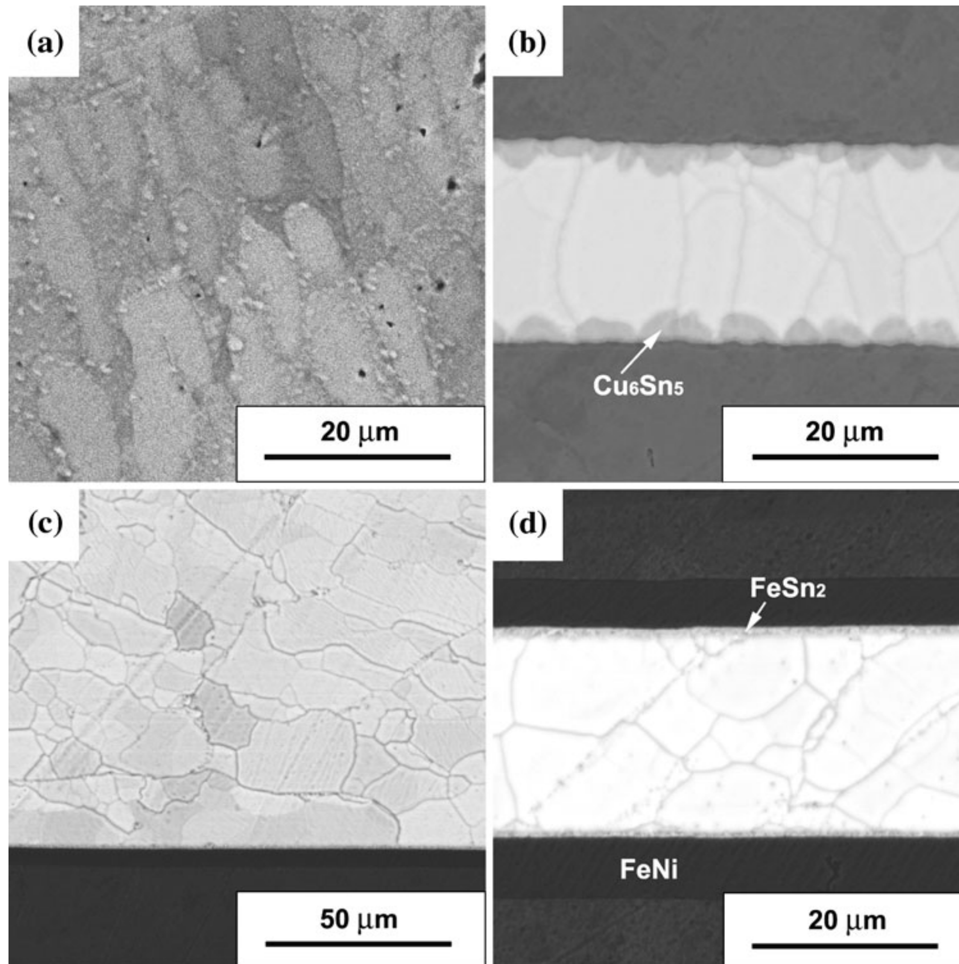

Fig. 3. Microstructure of solder joints: (a) Sn/Cu, 300 μm; (b) Sn/Cu, 20 μm; (c) Sn/FeNi, 300 μm; (d) Sn/FeNi, 20 μm.

than tin alloy solder. So, it is reasonable that the hardness of the Sn/Cu and Sn/FeNi joints showed some difference. However, the hardness values were equal for the same kind of joint, the gap size having very little influence.

It was reported that, for lap joint specimens in shear, strain tended to concentrate near the interface and decreased exponentially with distance from the interface.[20] At the initial deformation stage of lap shear joints, the grains near the interface deform first while the grains in the middle can accommodate the deformation through grain rotation or grain boundary sliding. At larger strains, the middle grains are deformed by dislocation glide to meet deformation continuity requirements. As can be seen in Fig. 4, the shear curves for the 50-μm and 20-μm joints were brittle with little plasticity, experiencing sudden failure as soon as the maximum load was reached. Systematic observation of the failure processes for the thin joint is shown in Fig. 5. When the displacement was less than 0.02 mm, the solder was still under elastic deformation. As the displacement reached 0.06 mm, obvious plastic deformation was seen, and surface grain boundary grooves appeared, which might develop eventually into a crack. As the displacement reached or exceeded 0.09 mm, at the maximum load point, interfacial crack propagated quickly and the joint failed. Thicker joint (300 μm) had a longer plastic flow stage.

DISCUSSION

As shown in Fig. 3, the microstructures for 300-μm and 20-μm Sn/Cu joints are different. During reflow, dissolution of Cu in the liquid Sn raised the Cu concentration as high as 1.4 wt.%, which is a hypereutectic composition. Under equilibrium cooling condition, the molten solder solidified in a wide temperature range (pasty range exceeds 30°C), and the normal microstructure consisted of some primary Cu_6Sn_5 particles, Sn dendrites, and (Sn + Cu_6Sn_5) eutectic phase. It was speculated that, under the quenching condition, the cooling rate was different for 300-μm and 20-μm solder joints. The volume for the 300-μm joint was 15 times that for the 20-μm joint, and the resultant cooling rate was slower. The 300-μm solder joint solidified into Sn dendrites and (Sn + Cu_6Sn_5) eutectic. However, in the 20-μm solder joint, which was subjected to large undercooling, Cu_6Sn_5 did not have enough time to

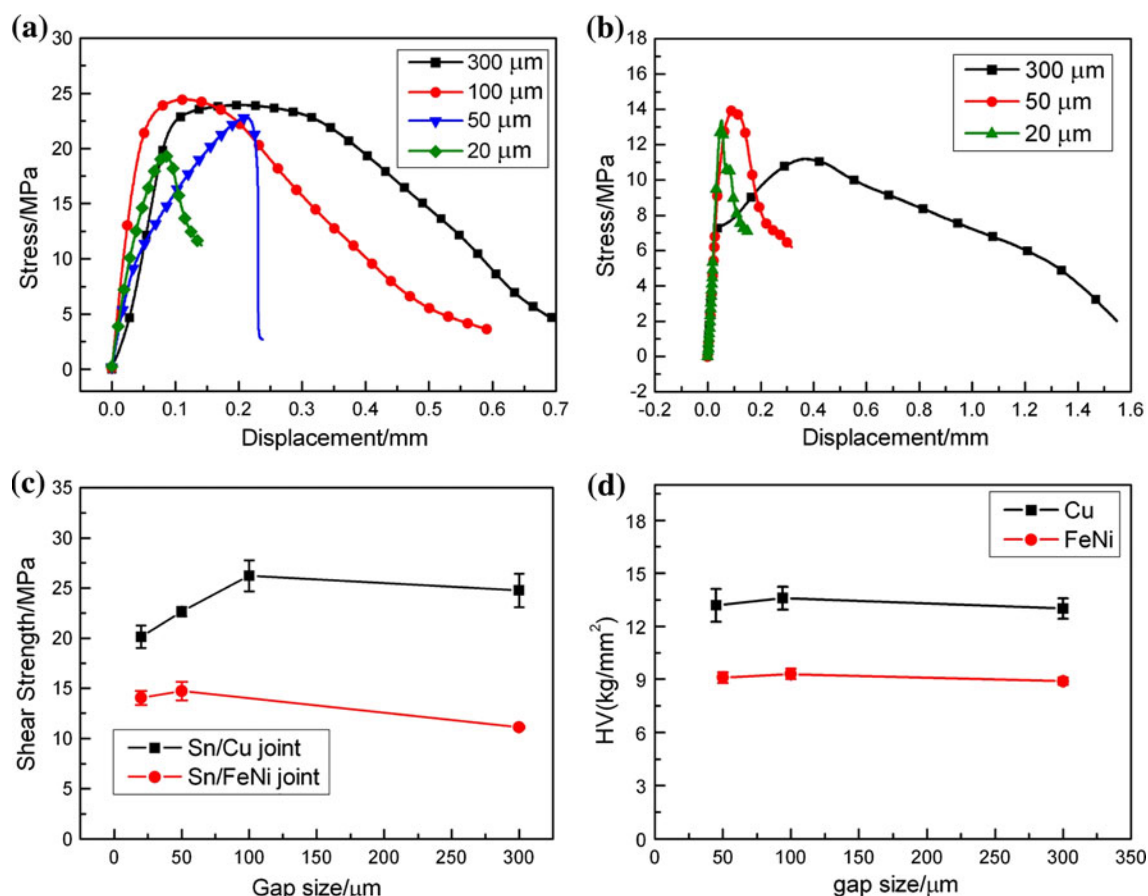

Fig. 4. Shear performance of solder joints at strain rate of 10^{-3}/s: (a) shear curves for Sn/Cu joints with different gap sizes, (b) shear curves for Sn/FeNi joints with different gap sizes, (c) ultimate shear strength for different gap sizes for Sn/Cu and Sn/FeNi joints, and (d) HV hardness for different gap sizes for Sn/Cu and Sn/FeNi solder joints.

precipitate in the solder. The solder solidified into a single β-Sn phase supersaturated with Cu. Consequently, only one layer of Sn grains appeared. In the Sn/FeNi joints with gap size ranging from 300 μm to 20 μm, the solder was close to pure Sn. During the cooling process, the freezing range was so narrow that a homogeneous microstructure developed easily.

As shown in Fig. 6, the fracture in the Sn/Cu joint with gap of 300 μm occurred inside the solder, and no interfacial failure was observed. In the Sn/Cu joint with gap of 20 μm, the fracture in the solder was near the solder/IMC interface and rotation of the Sn grains was clearly seen. The deformation of the Sn/FeNi joint was almost uniform across the solder. The fracture of the 300-μm and 100-μm joints followed a diagonal path across the joint, while for the 50-μm and 20-μm joints the fracture path was also found in the solder near the interface.

Since the fracture path observations indicated that all failure was controlled by the solder, it would be interesting to know the stress distribution in the Sn when the failure occurred. Finite-element analysis (FEA) was employed to evaluate the joint geometry effect on the stress distribution in the joint. In modeling the real test, one end of copper was fixed in all directions and the other end was pulled by a tensile force. In addition, to describe the plastic behavior of the solder, the Anand model[21] was used with the corresponding parameters listed in Table I. Only the elastic deformation was considered in the copper substrates, since the elastic modulus of copper is much larger than the value for solder.

Although the solder joint was considered in a shear stress state during testing, other components of stress may exist due to the shape of the specimen. To evaluate the stress distribution in multiaxial or complex stress states, the von Mises stress is usually used to compare with the tensile stress in the case of simple tension. The von Mises stress for pure shear stress expressed in three principal stresses is

$$\overline{\sigma} = \frac{\sqrt{2}}{2}\left[(\sigma_1 - \sigma_2)^2 + (\sigma_2 - \sigma_3)^2 + (\sigma_3 - \sigma_1)^2\right]^{1/2}. \quad (2)$$

The distribution of von Mises stress in the solder can be calculated and displayed directly in the powerful FEA software ANSYS12. The nominal stress applied at one end of the Cu was 20 MPa for general consideration.

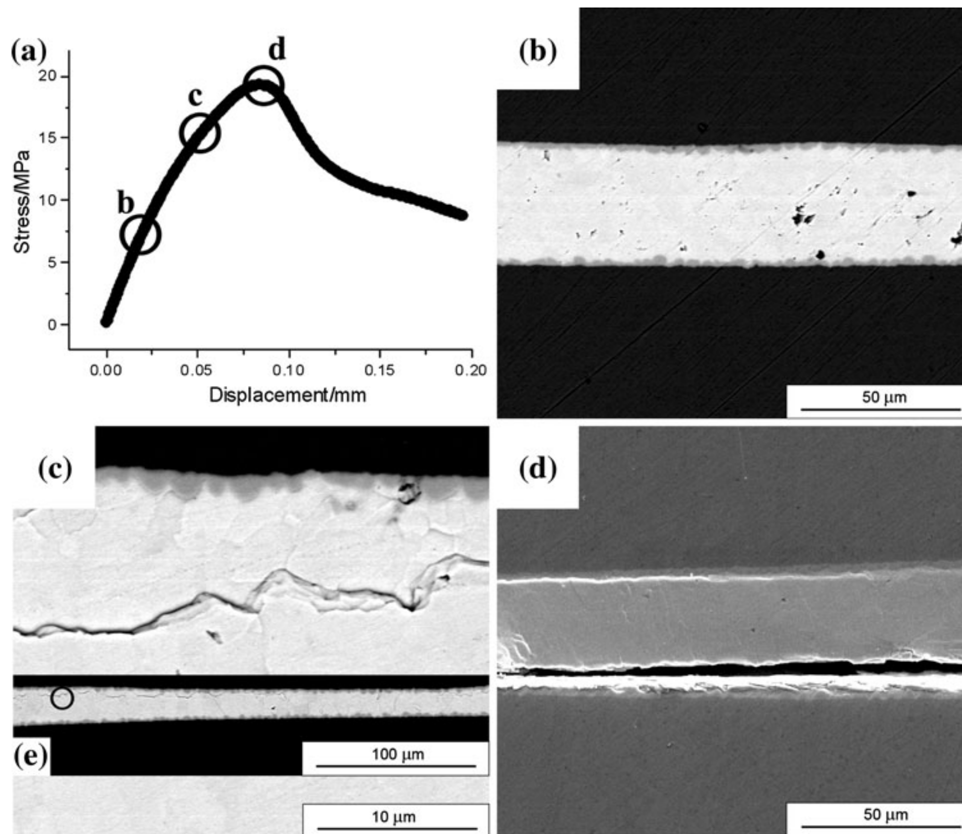

Fig. 5. Systematic observation of the failure processes for the 20-μm Sn/Cu solder joint. The morphology evolution of the solder joint corresponding to b, c, and d on the shear curve is shown in (b–d), respectively. (e, inset in c) Global view of the solder joint.

As illustrated in Fig. 7, the von Mises stress was uniformly distributed in the solder along the whole joint for the 300-μm solder joint. Small stress concentration zones with area less than 5% presented at the two ends of the solder. Although the stress distribution showed slight difference between the 300-μm and 20-μm joints, the maximum stress level inside the solder in both cases was almost the same. From our experimental and FEA results, it was clear that gap size, at least in the range from 20 μm to 300 μm that we investigated, has no obvious mechanical constraint strengthening effect on the shear strength.

It was easily concluded that the stress concentration zones would fail first before the average shear stress reached the failure shear strength, so that the overall load-carrying capability would be lower.[22] Such an effect seems to agree with the decrease of USS with decreasing gap size, as seen in the Sn/Cu system. However, in this work, the USS value of the Sn/FeNi joint had no obvious size effect. That means that the failure of solder joint is not sensitive to the local stress concentration in the solder, because the plastic deformation can accommodate the local stress concentration.

In the case of Sn/Cu joints, the microstructure of the 300-μm and 20-μm Sn/Cu joints was different, and the gap size effect might be induced by such microstructure variations. Yang et al.[11] reported a strengthening effect when the size of solder ball decreased, and ascribed the gap size effect to microstructural differences. As mentioned before, thicker Sn/Cu joints are characterized by a Sn + (Sn + Cu_6Sn_5) eutectic structure, while thinner Sn/Cu joints are associated with a single β-Sn phase. The eutectic phase can strengthen the solder more than solution strengthening. During deformation, Cu_6Sn_5 particles may anchor the dislocation movement. Precipitation of Cu_6Sn_5 at grain boundaries (GB) can also restrict grain boundary sliding or rotation. In the Sn/Cu joint with 20-μm gap, there were no Cu_6Sn_5 particles and dislocation motion would be much easier. As a result, dislocations would quickly move to the Sn/Cu interface and pile up to form microdefects which could initiate a microcrack. On the other hand, if the strengthening effect was nearly the same, for example, as in the Sn/FeNi joint, no gap size effect should be found, as observed experimentally. Therefore, the gap size effect found for the Sn/Cu system in this work can be attributed to the variation of microstructure with gap size. In fact, the microstructural variation may be induced by the gap size effect, because the dissolution of copper, liquid solder convection, and cooling rate may change with the gap shrinkage. For thinner solder joints, cooling in water was fast enough to prevent precipitation of the SnCu

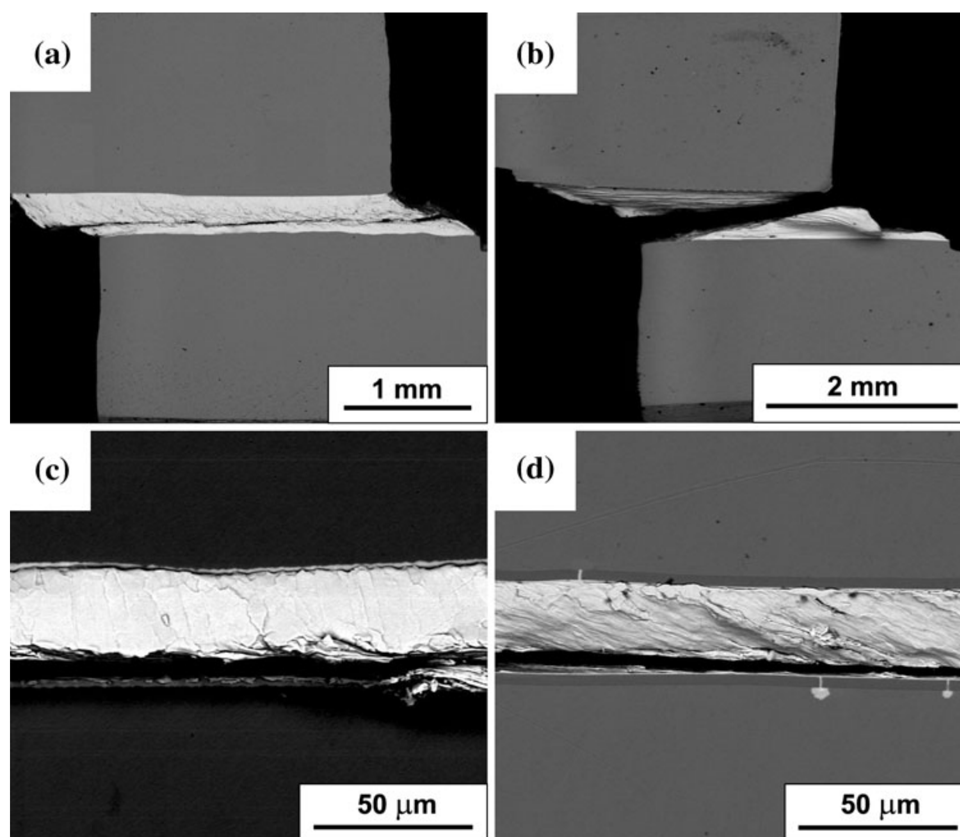

Fig. 6. Fractographs of: (a) Sn/Cu solder joint with gap size of 300 μm, (b) Sn/FeNi solder joint with gap size of 300 μm, (c) Sn/Cu solder joint with gap size of 20 μm, and (d) Sn/FeNi solder joint with gap size of 20 μm.

Table I. Parameters of Anand's model[21]

A (s^{-1})	Q/R (K)	ε	m	s' (MPa)	n	h_0 (MPa)	a	S_0 (MPa)
1.35×10^5	1.21×10^4	10.16	0.093	70.274	0.05	5.63×10^4	2.02	15.0

A pre-exponential factor, Q activation energy, R Boltzmann constant, ε multiplier of stress, m strain rate sensitivity of stress, s' coefficient for deformation resistance saturation value, n deformation resistance value, h_0 hardening constant, a strain rate sensitivity of hardening, S_0 initial value for deformation resistance.

compound and to form the single phase of the SnCu supersaturated solid solution. For thicker joints, the cooling rate was sufficient to produce (Sn + Cu_6Sn_5) eutectic phase.

CONCLUSIONS

Two kinds of solder joints (Sn/Cu and Sn/FeNi) were made with gap sizes ranging from 300 μm to 20 μm. Shear testing and FEA modeling were performed to investigate the gap size effect on the shear strength. Conclusions can be drawn as follows:

1. In the 300-μm Sn/Cu joint, (Sn + Cu_6Sn_5) eutectic structure developed, while in the thin Sn/Cu joint, only a single β-Sn phase was found. When the gap size went down to 20 μm, the solder microstructure was reduced to one layer of Sn grains. In contrast, dissolution of Fe and Ni in Sn was limited in the Sn/FeNi solder joint, and only a single β-Sn phase was formed regardless of the gap size.
2. The shear strengths of all the Sn/Cu joints were generally higher than those of Sn/FeNi solder joints. The Sn/FeNi solder joints exhibited roughly constant shear strength of 14 MPa with the gap change. However, the Sn/Cu joints exhibited a 20% reduction of shear strength with gap size shrinkage from 300 μm to 20 μm. The failures in all cases went through the solder instead of the IMC or solder/IMC interface. It

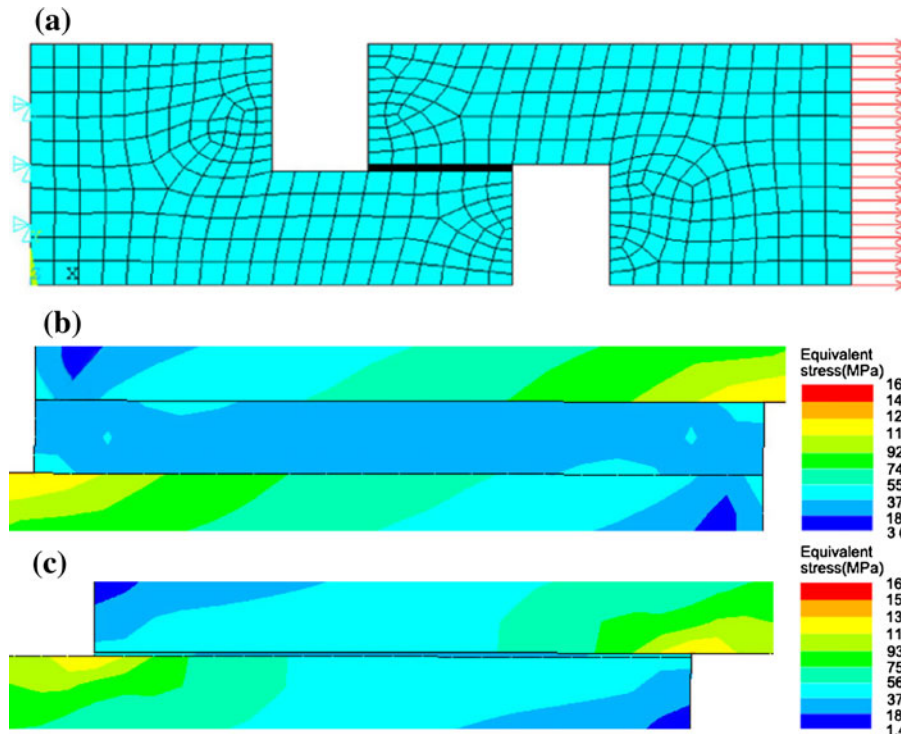

Fig. 7. Lap shear configuration and mesh detail used in finite-element simulations (a). A far-field load of 300 N is applied. This load level reached the USS in the solder joint (20 MPa). Contours of constant shear stress, σ_{xy}, in the solder and its vicinity for solder thickness of 300 μm (b) and 20 μm (c).

was implied that the shear strength of the solder joint still depended on the properties of the solder even when the gap size was decreased to 20 μm.

3. It was confirmed by FEA that the gap size shrinkage influenced the stress distribution but had very little effect on the stress level. For the Sn/Cu joint, the increase of shear strength with the gap size resulted from the presence of Cu-Sn intermetallic in the solder microstructure in the thicker joints.

ACKNOWLEDGEMENT

This work was financially supported by the National Basic Research Program of China (Grant No. 2010CB631006).

REFERENCES

1. Z. Zhang, D. Yao, and J.K. Shang, *J. Electron. Packag.* 118, 41 (1996).
2. Z. Zhang, J.K. Shang, and F.V. Lawrence, *J. Adhesion* 49, 23 (1995).
3. E. Orowan, J.F. Nye, and W.J. Cairns, *MOS Armament Res. Dept. Rep.* 35, 16 (1945).
4. Y.S. Lai, H.M. Tong, and K.N. Tu, *Microelectron. Reliab.* 49, 221 (2009).
5. S. Yang, Y. Tian, and C. Wang, *J. Mater. Sci. Mater. Electron.* 21, 1174 (2010).
6. P. Zimprich, A. Betzwar-Kotas, G. Khatibi, B. Weiss, and H. Ipser, *J. Mater. Sci.: Mater. Electron.* 19, 383 (2008).
7. Y.L. Shen, N. Chawla, and E.S. Ege, *Acta Mater.* 53, 2633 (2005).
8. N. Chawla, Y.L. Shen, X. Deng, and E. Ege, *J. Electron. Mater.* 33, 1589 (2004).
9. P. Zimprich, U. Saeed, B. Weiss, and H. Ipser, *J. Electron. Mater.* 38, 392 (2008).
10. P. Zimprich, U. Saeed, and A. Betzwar-Kotas, *J. Electron. Mater.* 37, 102 (2008).
11. J. Cugnoni, J. Botsis, and J. Janczak-Rusch, *Adv. Eng. Mater.* 8, 184 (2006).
12. J. Cugnoni, J. Botsis, V. Sivasubramaniam, and J. Janczak-Rusch, *Fatigue Fract. Eng. Mater. Struct.* 30, 387 (2007).
13. S.H. Yang, P.R. Lin, Y.H. Tian, C.Q. Wang, L. Liang, and Q. Wang, *8th International Conference on Electronics Packaging Technology* (ICEPT-HDP, 2007).
14. Y. Tian, C. Hang, C. Wang, S. Yang, and P. Lin, *Mater. Sci. Eng. A* 25, 468 (2011).
15. J.J. Guo, L. Zhang, A.P. Xian, and J.K. Shang, *J. Mater. Sci. Technol.* 23, 811 (2007).
16. C.W. Hwang, K. Suganuma, J.G. Lee, and H. Mori, *J. Mater. Res.* 18, 1202 (2003).
17. C.W. Hwang and K. Suganuma, *Mater. Trans.* 45, 714 (2004).
18. N. Dariavach, P. Callahan, J. Liang, and R. Fournelle, *J. Electron. Mater.* 35, 1581 (2006).
19. W.J. Tomlinson and A. Fullylove, *J. Mater. Sci.* 27, 5777 (1992).
20. X.W. Liu and W.J. Plumbridge, *J. Electron. Mater.* 32, 278 (2003).
21. L. Zhang, Z.G. Wang, E.H. Han, and J.K. Shang, *Constitution Behavior of SnAgCu Alloy*. Institute of Metal Research, unpublished (2006).
22. Y. Flom and L. Wang, *Weld. J.* 83, 32S (2004).